Self-correcting algorithm for estimated time of arrival of emergency responders on the highway

Self-correcting Algorithm for Estimated Time of Arrival of Emergency Responders on the Highway

Rreze Halili, Faqir Zarrar Yousaf, *Member, IEEE*, Nina Slamnik-Krijestorac, Girma M. Yilma, Marco Liebsch, Rafael Berkvens, *Member, IEEE*, Maarten Weyn, *Member, IEEE*

***Abstract*—Edge computing is one of the key features of the 5G technology-scape that is realizing new and enhanced automotive use cases for improving road safety and emergency response management. Back Situation Awareness (BSA) is such a use case that provides an advance notification to the vehicles of an arriving emergency vehicle (EmV). This paper presents an algorithm for enhancing the accuracy of the advanced Estimated Time of Arrival (ETA) notification of an approaching EmV towards the other vehicles on the highway. The notification is expected to ensure timely reaction by the vehicles to create a clear corridor for the EmV to pass through unhindered, thereby saving critical time to reach the emergency event in a safe manner. The main features of the presented solution are i) the self-correcting algorithm, ii) adaptive and dynamic dissemination areas size allocation, as a response to traffic changes, and iii) the evaluation of the ETA estimation accuracy.**

We have used the real travel time data measurements collected on the E313 highway (Antwerp, Belgium), to evaluate the performance of the algorithm. The performance is evaluated and compared in terms of accuracy and run-time complexity, using different methods such as Kalman filter, Filter-less method, Moving Average, and Exponential Moving Average filters. It is observed that the Kalman filter provides better accuracy on the ETA estimation, thereby reducing the estimation error by around 14% on average.

***Index Terms*—5G, C-ITS, C-V2X, ETA, MEC.**

I. Introduction

The latest advances in 5G technology enablers, such as Network Function Virtualization (NFV), Software Defined Networking (SDN), and Multi-Access Edge Computing (MEC) [1], are leveraged by vehicular networks in ways not perceivable before. These advances are expected to improve public safety in terms of avoidance of traffic accidents and improvement of emergency response time, considered as a lifesaving factor.

There is a significant research conducted to find a meaningful relationship between the emergency response time and the probability of fatal outcomes, and the results prove that the reduction of the overall response time plays a critical role in emergency situations [2–5]. For example, according to Sánchez-Mangas et al. [3], a 10 min reduction in the emergency response time decreases the probability of death by one-third. Although the regulatory requirements of some developed countries call for less than 10 minutes reaction time to life-threatening incidents, it becomes difficult to achieve especially during heavy traffic conditions.

The drivers mostly get informed about the presence of an approaching Emergency Vehicle (EmV) (e.g., an ambulance, a police vehicle, or a fire brigade) through blaring sirens and flashing lights. Since the drivers get alerted only when the EmVs are within their audio/visual range, they usually have a quite limited time and space to react and manoeuvre away from the path of the EmV in a timely, calm, coordinated, and safe manner. Creating a clear corridor for the EmV becomes more difficult and time consuming when there is high traffic density. This situation not only causes delays in emergency services response time but can also cause accidents. According to the report published by the National Highway Traffic Safety Administration (NHTSA) office of Emergency Medical System (EMS), 70% of all ambulance crashes occur while operating in an emergency mode [6], while Donoughe et al. [7] report that 66% of firetruck crashes occur when the truck is being used during an emergency.

To address the aforementioned challenges, a lot of research work has been done on modelling and optimizing the ambulance response time. As we discuss in Section II, most of the solutions propose methods calling for route optimization that enables the circumvention or avoidance of congested locations in order to ensure the timely arrival of the EmV to the intended destination. However, such solutions are limited, as they depend on the country, time of the day/year, weather, traffic conditions, and limited route options.

Given such limitations, we present a more universal Vehicle-to-Everything (V2X) method that leverages the MEC systems to generate and disseminate customized notifications on the EmV's arrival. The reason for proposing a Vehicle-to-Network (V2N) solution is the limited communication range of Vehicle-to-Vehicle (V2V) systems. In particular, the short-range communication generally refers to the distance below 1km, where V2V coverage is up to 300 meters [8], which is not enough for providing the drivers with the required time to calmly inter-coordinate between themselves and free the lane to create a safety corridor for the fast approaching EmV. Thus, our proposed Back-Situation Awareness (BSA) method enables an early notification of the Estimated Time of Arrival (ETA) of an approaching EmV, while it is still out of the audio visual range of the vehicles along its route-path.

As illustrated in Fig. 1, the BSA service instantiated within the MEC system [9] is able to parse the received ETSI Cooperative Intelligent Transport System (C-ITS) Cooperative Awareness Message (CAM) [10] notifications such as speed, location, direction, and destination of the EmV. Based on these parameters, the BSA service application derives the values of ETA from the EmV's current location with reference to the

Manuscript received September, XX, 2021; revised XXX, XX, 2021.

R. Halili, N. Slamnik-Krijestorac, R. Berkvens, M. Weyn, are with the University of Antwerp - imec, IDLab, Antwerp, Belgium, and F. Zarrar Yousaf, G. M. Yilma, M. Liebsch, are with the NEC Laboratories Europe GmbH, Heidelberg, Germany, (e-mail: rreze.halili@uantwerpen.be, zarrar.yousaf@neclab.eu, nina.slamnikkrijestorac@uantwerpen.be, girma.yilma@neclab.eu, marco.liebsch@neclab.eu, rafael.berkvens@uantwerpen.be, maarten.weyn@uantwerpen.be).

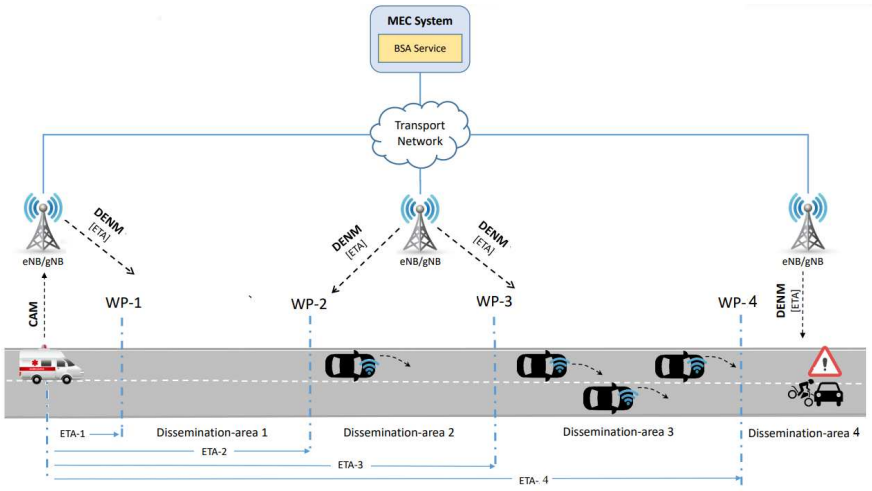

Fig. 1: Back Situation Awareness Overview.

respective Way-Points (WPs) specified by the BSA service application along the designated route-path of the EmV up until the EmV's destination. The values of ETA (displayed as ETA-1, ETA-2, ETA-3, and ETA-4, in Fig. 1) are encoded in the ETSI C-ITS Decentralized Environment Notification Message (DENM) [11] and disseminated to the vehicles within the respective dissemination areas. The areas, i.e., Dissemination Area 1, Dissemination Area 2, Dissemination Area 3, and Dissemination Area 4, are defined using the consecutive way-points referred to as WP-1, WP-2, WP-3, and WP-4, respectively.

This work extends our previous work [12] where a basic version of the BSA algorithm was implemented using Kalman filter [13] and analyzed using fixed dissemination areas. The analysis showed that the prediction accuracy of the ETA values is intrinsically linked with the size of dissemination areas, as well as the speed impacted by the traffic density in each dissemination area. The challenge, therefore, was to develop a BSA algorithm that is able to dynamically self-correct, taking into consideration the estimation errors values caused by the forecasting technique and dissemination area size, and the speed of the EmV, to predict accurate ETA values.

For this purpose, the scope of our research has been expanded beyond [12], which resulted in extending the BSA algorithm to take into account the prevailing traffic conditions and estimation errors when determining the optimal size of the dissemination areas that will give an accurate prediction of the ETA. This way, the algorithm is able to dynamically resize the dissemination areas in order to enhance the prediction accuracy. In addition, we perform a comparative analysis of accuracy and run-time complexity of different filtering methods to determine the one that gives more accurate prediction of ETA values, while using fewer processing steps. We also observe and discuss the impact that the frequency of the EmV input data has on the prediction accuracy when deriving ETA values.

The significance of this paper includes the development of a novel algorithmic solution to enable BSA service by leveraging the 5G MEC infrastructure. The proposed algorithm calculates the ETA of emergency vehicles and disseminates it among surrounding vehicles in the traffic. In addition, the proposed solution is a self-correcting algorithm that can identify and measure the prediction error and reconsider this for prediction accuracy improvement for the next steps. Furthermore, the proposed algorithm is able to dynamically resize the dissemination areas in order to enhance the prediction accuracy. The solution is expected not only to improve the road safety standards but also to enhance the mission success and response time of emergency responders.

For our analysis, we compare our results with the experimental data measurements reflecting the Actual Time of Arrival (ATA) obtained on the Smart Highway testbed[1] placed on the E313 highway in Antwerp, Belgium.

The rest of the paper is organized as follows. Section II provides Related work, followed by Section III presenting the use case of the BSA scenario and providing a system's perspective. Section IV gives details about the dynamic self-correcting algorithm for accurate ETA prediction and related concepts together with the filtering techniques. The analysis and performance evaluation of the ETA algorithm within the BSA application in terms of accurate calculation and dynamic dissemination of the ETA is provided in Section V, followed by Section VI concluding the paper.

II. Related Work

Along with the growing needs for transportation, the ever-increasing number of vehicles causes numerous issues on the roads and highways such as traffic jams, car crashes, fatalities, etc. Thus, most of the research efforts on the situation awareness in vehicular scenarios tend to analyze the methods that support the Emergency Management Systems towards reducing patient mortality, preventing disability, and improving chances of recovery [14]. One of the key factors for achieving these objectives is the emergency response time, which is considered as crucial for saving people's life. Thus, the relationship between the emergency response time and the survival rate has been part of different research works and some of them are presented in Table I and discussed as follows.

According to Nicholl et al. [15] a 10km increase in straight-line distance is associated with around a 1% absolute increase in mortality, while Pell et al. [16] concluded that reducing ambulance response times to 5 minutes could almost double

[1]Smart Highway: https://www.fed4fire.eu/testbeds/smart-highway/

TABLE I: Overview of related work.

Research direction		Works
non-V2X concepts	evaluation of the EMS performance	[15–18]
	prediction of the EmV's travel time	[19–21]
V2X concepts	V2V	[22–30]
	V2I	[31]
	V2N	[32]

the survival rate for cardiac arrests not witnessed by ambulance crews.

Different predictive models, filters, routing, and navigation systems are used together with large historical datasets collected on different cities to optimize the route which the EmV should follow to avoid traffic, to have an accurate time of arrival estimation for the body expecting at the emergency units, and to have an efficient way of utilizing emergency services and resources. The proposed solutions depend on the countries and also on the time of the day, year, weather, and traffic condition.

To optimize the configuration and operation of the emergency response time, Iannoni et al. [17] provide an extension of the hypercube model, combined with the hybrid genetic algorithms. The aforementioned study suggests the relocation of the ambulance bases and their area of work, as a way to reduce i) the average user response time, ii) imbalance of the ambulances' workloads, and iii) the fraction of calls not serviced within a predetermined threshold. Furthermore, Poulton et al. [18] present an application of a data-driven methodology for route selection and the estimation of arrival times of ambulances travelling with blue lights and sirens on. This methodology recognizes only historical data collected internally by the emergency ambulance services, thereby not considering any real-time information, traffic, or related context information retrieved from the external systems (e.g., traffic management systems, and cellular network services).

Regarding the communication technology, most of the research effort in enhancing situation awareness on the roads is focused on the Vehicle-to-Vehicle (V2V) technology (Table I), despite the disadvantage of the short-range emergency notifications. Among these works, an extensive effort has been conducted so far to reduce the delay of operation for emergency responders [22,23,31]. In their survey on urban traffic management system using wireless sensor networks [22], Nellore and Hancke recognize the schemes for prioritizing EmVs, as well as the congestion avoidance by decreasing the average waiting time for vehicles at the intersection, as a foundation for the future research. Tackling the intersection assistance systems, Joerer et al. [24] show that the current *state-of-the-art* congestion control mechanisms are not able to support the intersection assistance adequately, due to the lack of fine-grained prioritization among vehicles. Since these existing congestion control mechanisms provide an equal share of communication opportunities to all vehicles, not considering the difference of road traffic situations or individual vehicles such as an EmV, the exchange of the traffic information cannot be done in a timely manner. Therefore, Joerer et al. [24] propose an improvement, which allows vehicles in critical situations at intersections to be temporarily exempted from congestion control, enabling them to communicate with possible collision candidates more frequently, through the so-called beaconing solutions that rely on one-hop broadcasting and 802.11p technology [24].

One of the interesting features of broadcasting awareness messages is the dissemination of Time of Arrival (ToA) of emergency vehicles. This way, the surrounding civilian cars can anticipate at which moment they should clear the lane. Senart et al. [26] study a reliable mechanism for transmitting information about EmV's ToA, using a wireless medium, and a feedback system. In their work [26], Senart et al. proposed a method to disseminate information on EmV's arrival and to provide real-time feedback to EmV in case the quality of the communication is degraded. In this kind of scenario, the EmV will be informed that certain vehicles may not have been warned, thus receiving a recommendation to slow down. Other approaches for disseminating information about EmV are presented by Kapileswar et al. [27], Johnson [28], Metzner and Wickramarathne [30], and Hadiwardoyo et al. [29]. These studies rely on V2V connection to disseminate information on the location and the route path of EmVs in real time, in order to provide vehicles in a closer proximity with the EmV's arrival times, so that vehicles can adjust the driving decisions by considering the incoming alerts.

Nevertheless, as already mentioned, a drawback of the V2V communication is its short range (below 1km), which is not sufficient for the drivers to timely react and clear the lane for the approaching EmV. Thus, an attempt to utilize Vehicle-to-Infrastructure (V2I) communication is presented by Moroi and Takami [31]. To significantly decrease the travel time for EmVs, Moroi and Takami [31] proposed utilizing the Roadside Units (RSUs) that support EmVs by notifying other vehicles about the EmV's route.

The network infrastructure and vehicles need to react with the latency below 100ms [32] to achieve higher safety levels by being less dependent on the driver's actions. This of course requires service availability in the edges close to the vehicles. Due to a still limited range that they cover, most of the operational requirements for vehicular applications cannot be fulfilled by RSUs [33]. On the other hand, cellular technologies successfully cope with this challenge since base stations usually cover larger regions than the short range gateways (e.g., RSUs) [34]. Therefore, 5G systems supported by MEC are expected to improve the current support for V2X use cases [33,35], with the opportunity to significantly extend the notification range, and to decrease the delay by deploying vehicular applications at the network edge. By utilizing the cellular infrastructure, the management and orchestration entities, network controllers, and application services, are all fed with global information that helps them to notify civilian vehicles about emergency situations in extended regions, unlike in the case of short range communications where the local information in each vehicle does not include a broad view of the overall network.

It is in view of the above observations and shortcomings that we propose the BSA service the details of which are described in the subsequent sections.

III. Back Situation Awareness (BSA) Solution

A. BSA Use Case

As indicated above, the main objective of the BSA service is to improve the emergency response time, which is achieved by early notification/dissemination of the EmV's ETA to the vehicles, allowing them enough time to create a clear corridor for the EmV to pass through unhindered.

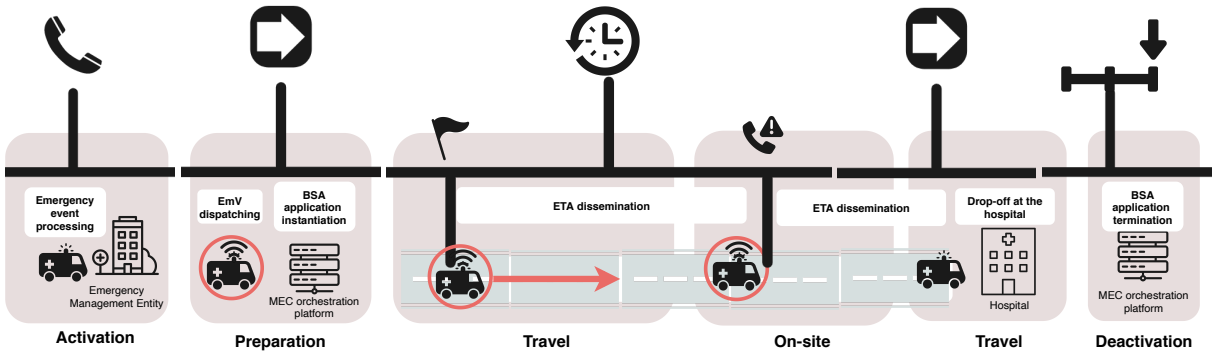

Fig. 2: Emergency response process with respective operations.

There are different definitions of the emergency response time. A general overview found in many standards defines the emergency response time as the overall time being comprised of four unique time intervals, which include the activation, response or preparation, on scene, and transport intervals [36,37].

As shown in Fig. 2, when the Emergency center is notified about an emergency event, we consider this as the activation time. Afterwards, the time which is required to dispatch an EmV to the emergency case is known as the preparation time. The time spend on the way to reach the destination is the travel time. The time spent on the event is the on-scene interval, and finally, the time spent from the ambulance departure to the hospital is the travel time. In each emergency response time interval, our BSA application running on the MEC system has its role, and uses its components and operations to initiate the algorithm, to calculate the ETA, to disseminate it on the upcoming route-path, and at the end to terminate the use of the ETA algorithm (see Fig. 2).

A high-level overview of the BSA use case is illustrated in Fig. 1. The event information is first received by an Emergency Management Entity (EME), such as 112 or 911 Headquarter (HQ), which dispatches an EmV providing it with the event location addresses or destination, the route-path to follow, and the IP address of the BSA service. While heading towards the destination, it will periodically start sending CAM via the mobile network infrastructure towards the BSA service instance, which is instantiated as a MEC application [9]. All the vehicles that are on the route-path of the EmV will process the received DENM notifications to extract the ETA values.

B. BSA Service Application Design

Fig. 1 gives the design overview of the BSA service application, which is envisaged to run as a Virtual Application Function (VAF) deployed and instantiated on the MEC system. Fig. 3 shows the functional elements that are chained to deliver the BSA service. In Fig. 3, we also depict the required interfaces enabling the BSA application to connect with the external entities. The interfaces A, B, and C are designed in a respective order to: i) receive upstream CAMs originating from the EmV with a specified frequency in Hz, ii) dispatch a DENM containing the derived ETA value for a specific dissemination area, and iii) maintain connectivity with a peering BSA application instance that may be running in another edge domain belonging to a different operator.

The EmV, after receiving the IP address of the MEC host where the BSA service application is instantiated from the EME, will start to transmit the CAMs periodically towards the BSA service on the MEC host. These messages will be received via the interface A, to be processed by the ITS protocol stack. In our case, this stack is provided by Vanetza, an open-source implementation of the ETSI C-ITS protocol suite [38]. The decoding function, which is a simple helper function supporting Vanetza, will parse, extract and filter the information relevant for the BSA algorithm from the CAM notification, and prepare an input parameters for the BSA algorithm, which are: i) the identification of EmV (EmV ID), ii) the speed of the EmV, iii) the current location of the EmV, iv) its destination, and v) direction of the EmV.

The BSA algorithm, marked in red in Fig. 3, is at the heart of the BSA service and the main contribution of this paper. It will calculate the ETA values for the respective dissemination area(s) each time it receives the CAM notification and will evaluate the estimation error, based on which it will take corrective actions for error minimization by readjusting the size of the dissemination areas. The details of the BSA algorithm are presented in Section IV while its performance analysis can be found in the Section V-B.

Along with the ETA calculation operations, the BSA algorithm stores the state of the application that refers to the information on the EmV's speed, location, and destination, in the state database (State DB in Fig. 3). The state database plays a significant role in the communication between two peering BSA service application instances running in two edge domains, thereby allowing them to share the EmV-specific meta information from one edge domain to the other via interface C (Fig. 3) or sharing data between different operators with different MEC systems. However, the coverage of multi-operator domains is out of the scope of this paper.

Furthermore, the output of the BSA algorithm, i.e., mainly the ETA values for respective dissemination areas is being processed by the ITS protocol stack, referred to as the Encoding Function in Fig. 3. This function has the task to prepare ETA notifications for the different dissemination areas by passing the information on: i) EmV ID, ii) calculated ETA value, and iii) dissemination area, to the transmit function of the Vanetza ITS protocol stack. The ITS protocol stack will encode this information in the DENM notification message, and dispatch it towards the mobile network infrastructure via interface B. This DENM notification is then disseminated (e.g., via broadcast) in the respective Dissemination Areas by the Dissemination

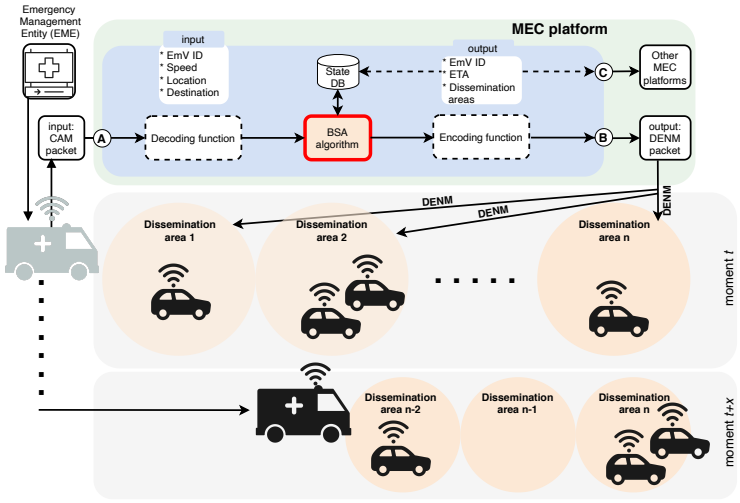

Fig. 3: BSA operation overview.

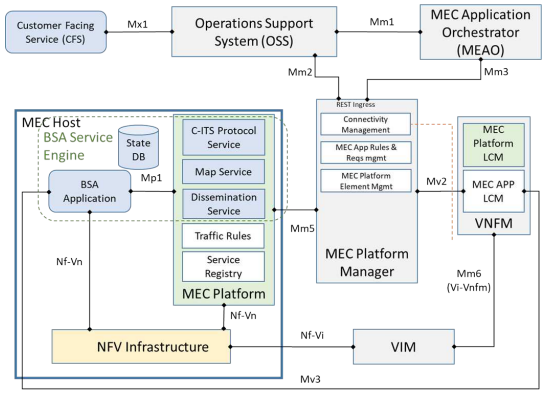

Fig. 4: BSA Service in the context of MEC system.

Service.

Each of the functional components within the BSA service is implemented as a visualized MEC service or MEC application, and thus instantiated on a MEC system. Fig. 4 gives the overview of the BSA service in the context of the standard ETSI MEC system architecture [9]. While BSA Application contains the logic of assigning WPs on the route-path and computing ETA values, C-ITS Protocol Service is used for decoding/parsing/encoding C-ITS CAM/DENM notification messages. Further, Map Service is used for getting geospatial information related to the route-path the EmV is traveling on, and State DB is proposed to store the meta-data/state-information of the EmV decoded/parsed/encoded CAMs/DENMs. Dissemination Service is used to broadcast the EmV's ETA information to the vehicles in front of the EmV within the relevant geo-casted dissemination areas.

The other functional elements shown in Fig. 4 are specified in the ETSI GS MEC 003 v2.1.1 standard [9] and are used for the management and orchestration of the BSA related MEC applications and MEC services. It should be noted that the EME is able to access the BSA system via the Customer Facing Service (CFS) interface. The details of the design of the BSA service components along with the details of the service orchestration and life-cycle management have already been described in our previous work [12].

IV. Estimated Time of Arrival Algorithm

A. ETA algorithm workflow

As described above, the BSA algorithm takes as inputs the location, speed, ID, direction, and destination (i.e., the location of emergency event) of the EmV for the calculation of the ETA values with reference to multiple WPs along the EmV's route path (see Fig. 3).

The workflow of the algorithm is shown in Algorithm 1. The BSA application is continuously listening to potential input information. In the case of the first received CAM, the message will be decoded and delivered to the BSA algorithm, which then analyzes the collected input data. The first step is to define the current geo-location of the reference object, which in our case is an emergency vehicle. Then, the algorithm checks the required destination and uses a Map Service to determine the route-path that EmV should follow while heading to this destination. Considering the route path determined by the way-points, the algorithm will derive the ETAs for all dissemination areas, and create an ETA vector that will be broadcasted to the vehicles in front of the EmV, using DENM and 5G mobile network infrastructure.

Depending on the frequency of input CAMs, which can be 1Hz, 2Hz, or 10Hz, the algorithm is obtaining the updated information every second, 500ms, and 100ms, respectively. With each upcoming CAM notification, the algorithm checks the position of the EmV, as well as the timestamp at which this position was recorded. We consider this value as the Actual Time of Arrival (ATA), which is further used to check the accuracy of the previously recorded and transmitted ETA. The difference between ATA and ETA for the considered location is presented as the estimation error, and is considered as a performance indicator, which is used as a feedback correction index for the following calculation of the ETA. Depending on the ATA value and the actual speed of the EmV, the algorithm determines the size of the dissemination areas, and the number of reference WPs. Note that the so-called estimation error can result in a different sign. It will be positive if the ATA $>$ ETA and vice versa.

The algorithm will continue updating ETA values for the (re-)defined dissemination areas until the EmV arrives at the destination. Once EmV reaches its destination, the whole

application, including the algorithm, will terminate and release the allocated MEC resources.

Algorithm 1: Workflow of the traffic signal for the main algorithm.

```
Result: Estimated Time of Arrival (ETA)
Start;
ϵ = 0sec ; step 1; while EMV Not arrived at Destination do
    Listen to arrival of CAM Notification;
    Get current geo-location of EmV;
    if EmV moved from previous position then
        Determine the Actual time of Arrival (ATA);
        ETA − ATA = ζ;
        if ζ ≠ ϵ then
            Go to step x;
        else
            Re-evaluate the number and size of
             dissemination areas and ETA values per
             dissemination areas; ETA_P = ATA;
            Derive/Adjust coordinates for each
             dissemination area;
            Go to step 1;
        end
    else
        Derive the ETA for all dissemination areas, and
         Create an ETA Vector;
        Disseminate the ETA Vector in each sector
         towards dissemination areas;
        if (EmV arrived) then
            Clear/Delete the previous dissemination
             area; Stop;
        end
    end
end
```

The reference scenario shown in Fig. 1 and Fig. 3 is modeled as a graph that consists of the route and the WPs. The sequence of the WPs (i.e., WP_1, WP_2,...WP_i) defines the size and the edges of the dissemination areas, and it represents the route-path that the EmV should follow.

Estimating time of arrival for different dissemination areas is based on the EmV's current location with reference to each WP (i.e., WP_i), and it is denoted as ETA_i. The sum of all travel times of consecutive WPs is considered to be the total time of travel. However, predicting the travel time is not straightforward, since the travel time in an urban traffic environment is highly dynamic, uncertain, stochastic, and time-dependant. Various factors such as random fluctuations in travel demands, weather conditions, interruptions caused by traffic control devices, incidents, etc., have an impact on the travel time [21,39]. Therefore, each WP_i is characterized with a distribution of ETA_i values, which implies an uncertainty on the total time of travel. According to Min et al. [21], this uncertainty is presented using a mean value $\mu(t_i)$ and a variance $(\sigma(t_i))^2$ of the ETA_i, as depicted in equations (1) and (2), respectively.

$$\mu(t_i^j) = \int_{t_1}^{\infty} t {F_i}^j(t)dt \tag{1}$$

$$\left(\sigma(t_i^j)\right)^2 = \int_{t_1}^{\infty} t^2 F_i^j(t)dt - \left(\int_{t_1}^{\infty} t^2 F_i^j(t)dt\right)^2 \tag{2}$$

The time t_1 in equation (1) represents the starting time of the trip, while $F_i^j(t)$ denotes the Probability Density Function (PDF) followed by the arriving time at the considered WP_i. The route-path that is followed by the EmV is indicated using j, however, in our case, the route path to the destination is determined by the MEC Map service, so we exclude it from the following expressions since j is a known pre-defined path. The uncertainty caused by the distribution of the ETA_i at any WP_i has an impact on the whole ETA calculation since it always depends on the distribution of the previous ETA_{i-1}. As denoted in equation (3) (see [21]), the ETA (t_{i+1}) distribution with reference from EmV's current position to a specific WP (WP_{i+1}), depends on i) the distribution of the ETA (t_i) for the previous WP, (WP_i), ii) the average speed of the EmV ($s_{v_i,v_{i+1}}(t_i)$), as well as iii) the distance between two successive WPs ($L_{i,i+1}$).

$$t_{i+1} = t_i + \frac{L_{i,i+1}}{s_{v_i,v_{i+1}}(t_i)}. \tag{3}$$

The distance is a constant parameter that depends on the route-path that the EmV selects to reach the destination. In our case, it is calculated using the WPs obtained from the MEC Map service (see Fig. 3) along the selected route-path. Following this approach, we assume that the variance of the ETA depends only on the variance of the average speed of the EmV. This approach emphasizes the importance of monitoring the variation of speed, which is directly impacted by the traffic conditions on the selected route-path.

Therefore, the uncertainty and time-dependent distribution - PDF of the speed, has an impact on the $F_i(t)$ calculation, which is used for calculating ETA. One example of performing the analytical relation of the PDF of ETA and the PDF of speed can be found in [21]. In this work ([21]) the information about the mean and variance calculated in equation (1) and equation (2) are used to select the shortest path to the destination by minimizing the mean and the variance of ETA_i [21]. Also, different studies [40–42] use mean and variance to investigate reliable routing optimizations. This approach is considered complex and time-consuming for real implementation [21], thus we propose a system that overcomes such a challenge in the following way. The BSA service is being constantly updated with the real-time speed and position information from the EmV, which ensures the accurate and real-time observation of speed and travel times. Also, the BSA service ensures in-advance notifications of the EmV's arrival time, thereby expecting from the vehicles in front to free the required lane for the EmV. In this situation, the proposed system can always select the shortest path, regardless of the traffic conditions, time of day/year, or other impact factors. Therefore, the average speed of the EmV, i.e., $s_{v_i,v_{i+1}}(t_i)$, refers to the value of speed maintained between the two successive WPs, i.e., WP_{i+1} and WP_i, and it is obtained from the periodic real-time CAMs, as well as the historical data collected during the previous traveling experiences on the same route-path.

In this study, we use real-time data for travel time prediction. Compared to different potential simulated models, this experimental approach is developed based on real dynamic travel

time data, which is a very important feature of this work. For this, we utilized the dataset that is collected from the field measurements of the vehicle driving on the Smart Highway testbed that is installed on the E313 highway in Antwerp, Belgium [43]. More details on the testbed are provided in Section V.

In particular, an important parameter such as the periodic real-time value of the speed is obtained from a Global Navigation Satellite System (GNSS) device that reports on the EmV's position, speed, and time. The values of speed are updated while the vehicle is driving on the selected path with the transmission frequency of 1 Hz. According to our analysis, this frequency of CAMs can be considered as high enough to enable our algorithm to derive values of ETA within the acceptable bounds of the ETA estimation error. More details on the error bounds are provided in Section V-B.

The considered historical data set is collected from the recorded journeys performed on the selected highway. As this data have the position, the speed, and the time, from the moment when this sample data was recorded, we created a matrix of data for the considered segment of the road. This matrix contains the estimated values for the average speed, and the travel times for the respective route segment, depending on the time of the day. Similar approaches are presented in different studies [18,44]. However, in the aforementioned studies, methods that are employed to estimate the speed and the travel require access to large capacity historical datasets from the emergency medical institutions to predict arrival times of ambulances in different parts of the cities/urban/rural areas. In our proposed solution, the matrix of the data is being constantly updated using the received CAMs from the EmV. Therefore, we expect that the matrix will contain timely updated accurate average speed values for 24 hours of the day, thus identifying rush hours, busy areas within cities, weather conditions, congestion, and ridership.

In our previous work [12], we used Kalman filter to estimate ETAs, utilizing the historical records of the measured values for the average, and the real-time speed received from CAMs. In this work, we enriched our experimentation with more measurements, and analyzed the three additional approaches, which filter the speed parameter for ETA estimation. We use i) the Filter-less method, ii) the Simple Moving Average Filter, and iii) the Exponential Moving Average Filter. The key objective of adding and assessing these three simple filtering methods is to analyze if we can obtain the required accuracy with the reduced costs and complexity of the algorithm, compared to the Kalman Filter.

B. Overview of the reference methods

To compare and assess the resulting ETA accuracy, four different forecasting methods are used.

1) Filter-less method: When using the filter-less method, a speed value (v[n]) obtained from a single CAM notification (without taking into consideration the previous speed data), is considered to calculate the ETA.

In case of the ETA defined in the equation (3), the average speed $s_{v_i,v_{i+1}}(t_i)$, can be obtained via a discretized method (equation 4).

$$s[n] = v[n]. \tag{4}$$

This way, anytime the BSA application receives a new CAM notification, it will consider the reported speed $v_i(t_i)$ (or v[n]), and calculate the ETA value for the upcoming way-points on the highway while the EmV is heading towards the emergency case.

2) Simple Moving Average Filter: The Simple Moving Average, as the name indicates, is an average that moves. The average is created using older data in combination with the newly available data, causing this parameter to move along the time scale.

When using this method, the speed parameter $s[n]$ is formed by computing the average speed of the EmV over a specific period, which we define as a window size. In our case, we have considered a window size (N) equal to 5, which means that the average speed $s_{v_i,v_{i+1}}(t_i)$ in equation (3) is calculated based on the last five values of speed reported by the EmV.

$$s[n] = \frac{1}{N} \sum_{i=0}^{N-1} v[n-i] \tag{5}$$

As shown in the equation (5), if the Simple Moving Average filter is used, the average speed is derived from the sum of the values divided by the number of values.

3) Exponential Moving Average Filter: Same as in the case of the Simple Moving Average, the Exponential Moving Average filter follows the logic of moving average. However, in this case, the resulted average speed depends on the previous average and the current speed value. The filter is called *exponential*, because it uses an exponentially smoothing factor α to include the weight of the previous input speed values (equation 6).

$$s[n] = \alpha \sum_{i=0}^{N} (1-\alpha)^i v[n-i] \tag{6}$$

4) Kalman filter: As reflected in the literature [19,20,39,45–47], Kalman filter has been extensively used in numerous traffic-related studies that have investigated travel time estimation for different practical applications. Different studies reveal that Kalman filter can perform a highly accurate estimation and performance analysis of the estimators, due to its performance and its effectiveness in continuously updating the state variable - prediction with real-time measurements. Furthermore, the ability of the filter to combine the effects of noise of both the process and measurements, in addition to its computational approach, has made it very popular in many research fields [45]. The study provided by Chien and Kuchipudi [39] reveals that Kalman filter performs better compared to various time series models and artificial neural network models. Although the aforementioned prediction methodologies use speed, volume, and occupancy data, as an input, the results show that they are most-likely site-specific, which makes them inapplicable to more generic scenarios. Thus, using the same methods on another site or with other traffic conditions lead to decreased accuracy in prediction. On the other side, Kalman filter combines the use of historic path-based data and continuously updates on the traffic behavior. This provides better accuracy especially during peak hours due to smaller travel-time variance, and the larger sample size [39]. Same conclusions are found also in [19], where Kalman filter is developed to predict the traffic flow. According to Emami et al. [19], Kalman filter has an acceptable accuracy to predict the traffic flow even in the presence of abrupt changes in traffic conditions. In [45],

Shalaby and Farhan show that Kalman filter outperforms other traditional models (i.e., regression and neural network models) in terms of accuracy, demonstrating the dynamic ability to update itself based on new data that reflects the changing characteristics of the operating environment.

In this study, we use Kalman filter to estimate the travel time, as this type of filter enables combining the prediction of the ETA with the real-time arrival times observations obtained from the periodic real-time CAM messages. In addition, the historical data on the travel time, collected for the studied route paths, are included to improve this estimation.

This filter consists of the initialization, prediction, and correction steps, for every input value, and it uses linear stochastic difference equations to estimate values of interest [48].

The considered state and measurement models are also presented in our previous work [12], where in the equation (7), $\underline{x}_k$ is the state variable, which is in our case the ETA for the respective WP_i. Then, A is the state transition constant, which relates the present state $\underline{x}_k$ of the ETA to its previous state $\overline{x}_{k-1}$, calculated for the previous WP_{i-1}. Since ETA is a one-dimensional value, A is equal to 1.

$$\underline{x}_k = A\overline{x}_{k-1} + Bu_{k-1}. \tag{7}$$

Furthermore, the parameter B associates the control input parameter u to the ETA value of the step k ($\underline{x}_k$). Since the input u is the time interval added to the ETA of the step $k-1$ ($\overline{x}_{k-1}$), this input parameter is one dimensional as well, thus B=1. The control input u is calculated considering the segment's length L between WP_i and WP_{i-1} found on the the pre-selected route-path obtained from the mapping system, divided by the input speed parameter received continuously using CAM message. In order to include the impact of the process noise, we use covariance Q, thereby obtaining the covariance matrix P_k.

$$\underline{P}_k = A\overline{P}_{k-1}A^T + Q. \tag{8}$$

For the correction step, we consider the real data measurements and follow the equations (9)-(11). In our case study, the real-time CAM messages, as well as the historical data measurements, are used to obtain the vector of the ETA measurement values expressed as z_k, for the respective segments of the highway. The transformation matrix H is equal to 1 in our case, and $\underline{x}_k$ is obtained using equation (7). The obtained measurements include noise or uncertainty, whose variance is R [12]. The Kalman gain K, expressed in equation (9), determines to what extent the predictions should be corrected in time step k. This estimation/prediction error is the difference between the predicted value and the actual measurement. Depending on the value of variance measurement noise R, this gain gives weight to the predicted or the measured value. A large value of R results in the small K, which means that the predicted value does not reflect the measured one. On the contrary, if R is small, it means that the measurements for the specific area are approximated with an insignificant error value.

$$K_k = P_k H^T (H\underline{P}_k H^T + R)^{-1}. \tag{9}$$

$$\overline{x}_k = \underline{x}_k + K(z_k - H\underline{x}_k). \tag{10}$$

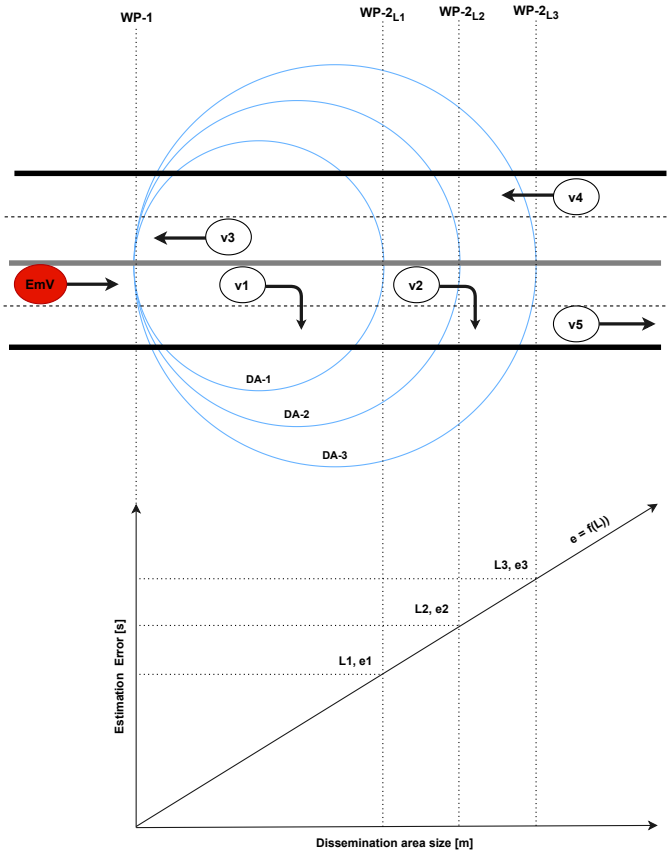

Fig. 5: Estimation error e dependency on the dissemination area sizes L.

$$P_k = (I - K_k H)\underline{P}_k. \tag{11}$$

C. Dissemination area size determination

As described in Section III, the BSA service determines the EmV's ETAs with reference to different WPs along the route-path, and then disseminates the calculated ETA values in respective dissemination areas. A dissemination area is defined as a region between two specific WPs, and the ETA is derived with reference to the WP marking the beginning of each dissemination area. Thus, all vehicles within the respective dissemination area will receive the same ETA value. As a result, besides the prediction error which is an outcome of the above mentioned forecasting techniques, the ETA value will be impacted by another estimation error ($e(t_i)$) within a dissemination area (i), which depends on the size (i.e., road-length) of the dissemination area (L_i).

In our previous work [12], we provided an empirical evidence of the effect of dissemination area size (i.e., L) on the estimation error (i.e., e_i). From the obtained results, we could see that the maximum estimation error of 62.22s was obtained for L=250m as compared to 92.10s observed for L=500m, and the maximum value of the estimation error, i.e., 118.08s, observed for L=1000m [12].

Thus, the larger the size of a dissemination area is, the larger the estimation error. The error behavior and its dependency on the dissemination area size are used to model, predict, and to limit it under a defined threshold suitable for an emergency

situation. In this regard, our analysis and observations of the data acquired from the real experimental drives, show a relation between the estimation error ($e(t_i)$) of the ETA value, the dissemination area size (i.e., road-length) ($L(t_i)$), the speed of the EmV ($v(t_i)$), and the index ($n(t_i)$) that is expressed in equation (12). The index n reflects the traffic conditions, weather conditions, time of the day/year, and other parameters that may impact the speed of the EmV.

$$e(t_i) = f(L(t_i), n(t_i), v(t_i)). \tag{12}$$

Fig. 5 illustrates the impact of the size of the dissemination area (L_i) on the estimation error, where the dissemination area is defined between WP-1 and WP-2. The figure shows that the magnitude of error value is proportional to the size of the dissemination-area $DA-1$, $DA-2$, $DA-3$, characterized by a linear increase in the estimation error as the size of the dissemination area increases from L_1, through L_2, to L_3, respectively. The slope of the estimation error is positive, and is defined by the change in the ATA parameter divided by the corresponding change in the distance parameter between two distinct points on the highway segment. As illustrated in in Fig. 5, the ETA error will be higher for vehicles that are farther away from the reference WP (i.e., WP_1 in Fig. 5).

According to our analysis and observations of the data acquired from the real experimental drives, the index n has a mean value of 1.07, minimum 0.01, maximum 1.41, and a maximum standard deviation of 0.47. Furthermore, this index has a tendency to exhibit very small changes between two successive calculations of ETA, thus it has a negligible effect on the two successive errors estimations. This makes it possible to use the previous value of the estimation error index $n(t_i)$ for the proceeding estimation error index $n(t_{i+1})$.

Therefore, for each newly received CAM, we use the relation between ATA_i, speed of the vehicle $v(t_i)$, and the distance d_i, obtained at the time t_i, as represented in equation (13), to forecast the index n for the upcoming time t_{i+1}.

$$n(t_{i+1}) = ATA_i \frac{v(t_i)}{d_i}. \tag{13}$$

The dynamically changing index n from every newly received CAM is used to dynamically adjust the dissemination areas sizes $L(t_{i+1})$ (see equation (14)), so that the estimation error caused by this size stays under a defined threshold (e_{i+1}^{max})

$$L_{i+1}^{max} <= e^{max}(t_{i+1}) \frac{v(t_i)}{n(t_{i+1})}. \tag{14}$$

The numerical value of the threshold $e^{max}(t_{i+1})$ is the maximum estimation error, which is allowed at the end of the generated dissemination area (i.e., numerical value of e_1 if L_1 is selected, or e_2 for L_2, or e_3 for L_3, in Fig. 5).

V. Performance Evaluation

We evaluated the performance of the BSA algorithm using a the case study presented in Section III, thereby including the four studied reference methods. The performance evaluation is made by measuring the accuracy of the ETA estimation, thus analyzing the parameters that impact this accuracy, with reference to the real data measurements presented in Section V-A.

Fig. 6: The segment of the two way E313 highway in Antwerp, Belgium. © 2020 Google.

Fig. 7: The OBU Roof Unit placed on the vehicle roof and the OBU Car Unit placed inside of vehicle.

A. Experimental testbed for reference data collection

In order to analyze the performance of the four reference methods in terms of accurate calculation of ETA, a real dataset was used as a reference. This dataset consists of the test data that has been acquired by driving a test vehicle on the selected segment of the E313 highway in Antwerp, Belgium (see Fig. 6), where the Smart Highway Testbed is installed. Besides parameters such as location and speed, the test data captures also the ATA of the test vehicle.

The testbed infrastructure, which is part of the Smart Highway, consists of the following interconnected hardware entities: a vehicle equipped with an Onboard Unit (OBU), the backbone, the testbed management software platform, and the optical fiber ring along the E313 highway.

As shown in Fig. 7, one part of the OBU is placed on the roof of the vehicle (1.8 m from the ground), and it contains an accurate GNSS module AsteRx-m2a with Real-time kinematic positioning (RTK) correction, and two GNSS PolaNt-x MF antennas. The second part of the OBU is placed inside of the vehicle, and it contains a processing unit with an independent power system, which can power the OBU for several hours. This device records the position of the vehicle expressed by its latitude and longitude with a predetermined frequency of updates, the time-stamp when this position is obtained, the precise and reliable heading information, and the vehicle's speed. These parameters are identified using an ID and are stored for post-processing.

The data measurements are obtained at different hours of the day, months, and years, making us able to evaluate the ETA performance under diverse traffic conditions. The travel-time data are collected in November 2020, (2020-11-19, 14:00 to 17:00 CET), June 2019 (2019-06-18, 14:00 - 15:00 CET), and July 2019, (2019-07-17, 12:00 to 14:00 CET).

Fig. 8 shows the sample of the 10 test drives, including

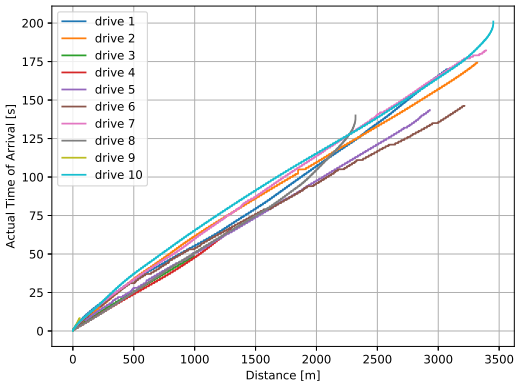

Fig. 8: Real measured travel time, referred as Actual Time of Arrival of the OBU while driving on the E313 Highway.

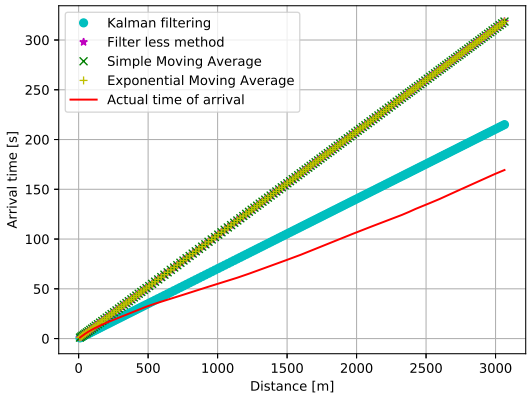

Fig. 9: Comparison of the real measured travel time ATA and the ETA values derived using four reference methods and information received from the first CAM notification only.

the time-stamp for each recorded position, which is then used as the ATA of the vehicle in our algorithms and analysis. As it can be seen in Fig. 8, the speed of the OBU changes, thereby resulting in different arrival times in different sections or distances from the starting point.

B. Results and Analysis

The main goal of this work is to evaluate the performance of the BSA algorithm in terms of the following key objectives:

1) Comparing the performance of the four reference methods in terms of their accuracy.
2) Determining the dissemination area size in order to obtain ETA estimation errors under an acceptable limit.
3) Analyzing the impact of the CAM input frequency on the ETA estimation error.
4) Comparing the performance of the four reference methods in terms of their complexity.

Thus, in the following sections, we present and discuss the obtained results, thereby pursuing the aforementioned objectives.

1) Accuracy of filtering methods: To analyze the accuracy, we use KPIs such as minimum/maximum/average/standard deviation of the estimation error. To compare the predicted values of ETA with the measured values (i.e., ATA), we use the following KPIs: Mean Absolute Error (MAE), Mean Absolute Percentage Error (MAPE), and Root Mean Square Error (RMSE).

In our analysis, MAE is used for obtaining the natural average magnitude of the absolute estimation errors by giving the same importance to each error. Furthermore, MAPE is used to express the accuracy as a percentage of the error, i.e., as the sum of the individual absolute estimation errors divided by the respective ATAs. Finally, the RMSE gives more importance to more significant estimation errors, i.e., higher deviations from the measured values. Thus, by considering these three KPIs, we have a complete picture of the estimation error distribution.

The datasets that are obtained from the field tests and described in the Section V-A, are used to analyze the difference between the measured values of ATA, and the values of ETA that are calculated using the four reference methods. In particular, to collect the measurements for the ATA values, we have used one of the OBU drives shown in the Fig. 8.

As already explained, the algorithm is generating new ETA values with every CAM that is received from the EmV. In particular, Fig. 9 presents the initial ETA values that are generated for all points on the selected path (i.e., starting from the EmV's initial position to its destination), taking into account the position, speed, and heading, of the EmV, which are stated in the first received CAM. In Fig. 9, we compare the predicted values (i.e., ETAs) derived using the four reference methods with the real time of arrivals (i.e., ATAs) recorded by the GNSS receiver, when the EmV is located at the starting point of the journey, and has a long distance in-front toward the destination.

We can see in Fig. 9 that the estimation error increases with distance, as the ETA diverges more and more from the ATA. As it can be seen, all methods are overestimating the arrival time of the EmV for the areas that are more than 600m away from the EmV's current location. In this case, the EmV will reach the vehicles at the front much earlier than the ETA notification stated, thus giving drivers limited opportunity to safely maneuver away from the EmV's path. Our solution prevents such scenario, since our algorithm is being constantly updated with the CAM notifications, thereby ensuring the update of ETA values along the path as well.

Furthermore, Fig. 9 shows that Kalman filter is deriving ETA values more accurately, i.e., the derived ETA values are closer to the measured ATA values, compared to the other three reference methods. Here we can clearly see the importance of the adaptive and self-correcting feature of the Kalman filtering that adjusts itself during the drive, whereas such feature is not present in the other three reference methods.

The difference between the measured ATAs and the generated ETAs can be observed as a vector with a certain distribution of the estimation error. Thus, in Fig. 10, we show how the maximum, the minimum, the average, and the standard deviation, of the estimation error change during the entire journey (from the EmV's starting point until it reaches the destination), in case Kalman filter is used for predicting ETA. In this case, the algorithm is being updated with the new input data every second, but the results are plotted every two seconds to achieve better visibility.

For every box plot representing the resulted vector in Fig. 10, we can see the peaks of estimation errors (both positive and negative). These peak values of the estimation error are obtained for the locations/distances that are far in-front from

TABLE II: Comparison of the estimation error obtained at d_0, d_1, d_2, d_3 using different techniques and different performance criterion.

Distance traveled d_i, Dissemination area size L	Prediction Technique	Min	STD	Max	Average	RMSE	MAE	MAPE (%)
d_0=9.5m, L=1000m	Kalman Filtering	0.072	21.94	54.46	9.38	23.86	19.55	41
	Filter less method	0.009	47.02	147.57	-27.15	54.30	44.77	62
	Simple Moving Average	0.009	47.02	147.57	-27.15	54.30	44.77	62
	Exponential Moving Average	0.009	47.02	147.57	-27.18	54.30	44.77	62
d_1=710m, L=335m	Kalman Filtering	0.086	7.00	28.90	11.33	13.32	11.38	20
	Filter less method	0.009	9.50	37.48	16.98	18.42	16.04	31
	Simple Moving Average	0.015	9.16	37.92	-27.15	18.68	16.28	33
	Exponential Moving Average	0.004	8.91	36.99	15.77	18.12	15.77	33
d_2=1598m, L=380m	Kalman Filtering	0.012	6.44	24.64	12.15	13.75	12.36	25
	Filter less method	0.010	6.44	24.55	12.10	13.71	12.10	33
	Simple Moving Average	0.040	6.64	26.43	-27.15	14.66	13.07	35
	Exponential Moving Average	0.035	6.60	26.11	12.90	14.49	12.90	34
d_3=2361m, L=375m	Kalman Filtering	0.061	6.40	22.15	11.57	13.22	11.57	29
	Filter less method	0.014	6.38	22.05	11.03	12.74	11.03	35
	Simple Moving Average	0.071	6.41	22.39	-27.15	13.34	11.70	37
	Exponential Moving Average	0.06	6.40	22.13	11.65	13.22	11.66	36

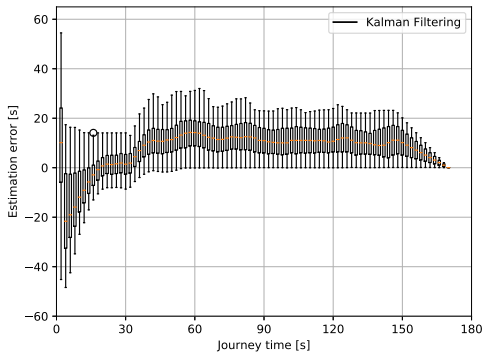

Fig. 10: Estimation errors obtained on different locations/distances toward the emergency case when using Kalman filtering.

the EmV's current location (as shown in Fig. 9). When using Kalman filtering technique, the accuracy of the algorithm is high for shorter distances, i.e., for those areas that are less than one km away from the Emv's starting point). When the distance increases above 1km, the estimation error also increases (as shown in Fig. 9). However, this does not affect the overall prediction accuracy, as the ETA values are being re-calculated every second with each new CAM notification, which in the end results in an improved accuracy. This is the first advantage of our solution compared to existing systems.

Also, while the EmV is moving toward the destination, the prediction distance decreases, therefore the estimation error decreases as well. This is reflected in Fig. 10, where we can also see that at the end of the journey the range of the estimation errors gets smaller (especially in the last area, i.e., when the journey time is between 150s and 180s).

Furthermore, Fig. 11 shows the comparison of the estimation error vectors obtained using all four methods, i.e., Kalman filtering, Filter-less method, Simple Moving Average Filter, and Exponential Moving Average Filter. The KPIs such as maximum estimation error, MAE, and RMSE, shown in Figures 11a, 11b, and 11c, respectively, are calculated for the entire distance, i.e., the entire journey time that the EmV travels toward the intended destination. The results show that the prediction accuracy of all methods increases as the distance from the destination drops, also confirming that the Kalman filter performs better in case of long distance predictions, compared to the other three reference techniques.

Same observation is shown in Table II, where we present the detailed numerical results for all four considered techniques, defining four different scenarios with reference to the EmV's distance from the starting point. Thus, the KPIs listed in Table II (i.e., standard deviation, mean, minimum , maximum, RMSE, MAE, and MAPE), describe the estimation error vector obtained when the EmV is located at the certain distance (i.e., d_0, d_1, d_2, and d_3) from the starting point. In particular, MAPE is reflecting how the algorithm performs in general when the EmV is at the certain distance from the starting point, by considering all vectors of estimation errors that are obtained while the EmV is heading towards the designated locations (d_0-d_3).

When the EmV sends the first CAM notification at the start of its journey, i.e., at the position d_0, the maximum estimation error is 54.46s for Kalman filtering, and 147.57s for other three methods. As it can be seen from the Table II, in case of d_0, MAPE is 41% for the Kalman filter, and 62% for other techniques, which shows that Kalman filter achieves 21% lower estimation error than the other methods. Considering other distances, Kalman filter keeps outperforming other methods, thereby achieving (11-13)%, (8-10)%, and (6-8)%, lower MAPE in case of d_1, d_2, and d_3, respectively.

2) Optimal size of dissemination areas: Moving to the second objective of this work, it is important to stress that in addition to the estimation errors inherently caused by the considered filtering methods, the size of dissemination area has an impact on the magnitude of the estimation error as well.

Given that we share a single ETA value for all vehicles located within a single dissemination area, it is intuitive that the estimation error is the lowest at the beginning of the dissemination area. This error increases for those vehicles that are farther from the start of the designated dissemination area, i.e., the closer they are to the end of the area, the larger the estimation error is.

In the very first step, our algorithm sets 1000m to be the default value of the size for each dissemination area, and then it dynamically changes the size with reference to i) the EmV's speed, which is extracted from the periodic CAM notifications, and ii) the upper error threshold (see eq. 14). With such approach, the dynamic definition of sizes with each newly

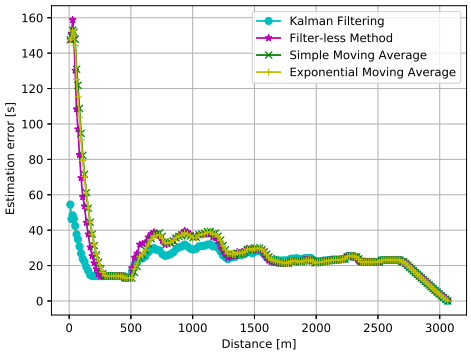

(a) Maximum estimation error values.

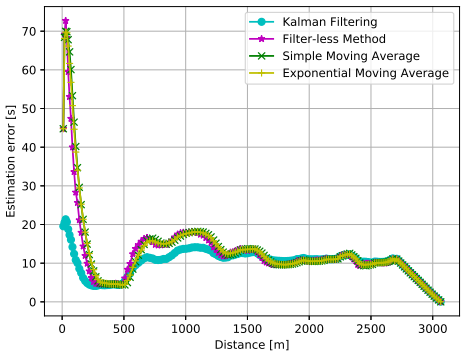

(b) Mean Absolute Error values.

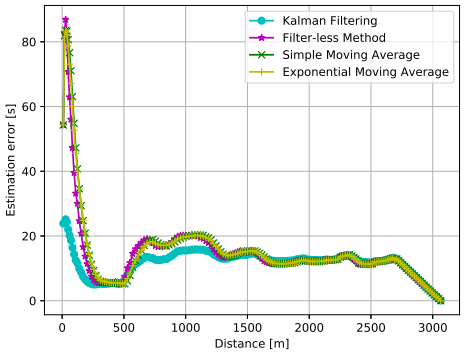

(c) Root Mean Square Error values.

Fig. 11: Comparison of the estimation errors obtained on different locations/distances toward the emergency case for the considered techniques and for the entire journey.

received CAM notification results in an increased estimation accuracy. Referring to Kalman filtering results shown in Fig. 11, the minimum estimation error after receiving the second CAM notification tends to be zero, while the maximum error is around 18s at the end of the first dissemination area (determined or limited by the threshold value), and 47s at the end of the journey (in our case more than 3km far from the current EmV location). Although the error is 47s for the end point of the journey, each new derivation of ETA will improve the accuracy, thereby updating the civilian cars with newly calculated values of ETA for their respective dissemination areas.

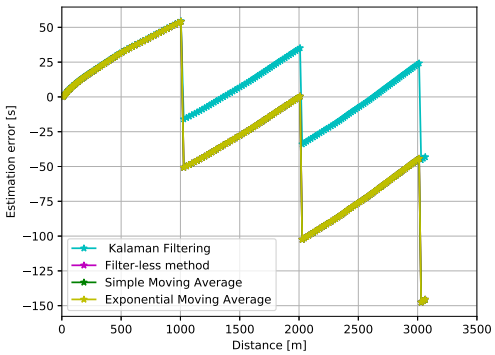

(a) e, d_0 = 9.5m, L = 1000m.

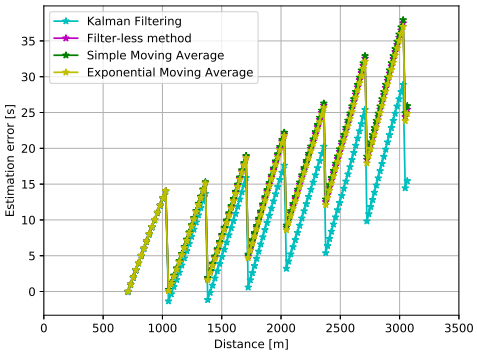

(b) e, d_1 = 710m, L = 335m.

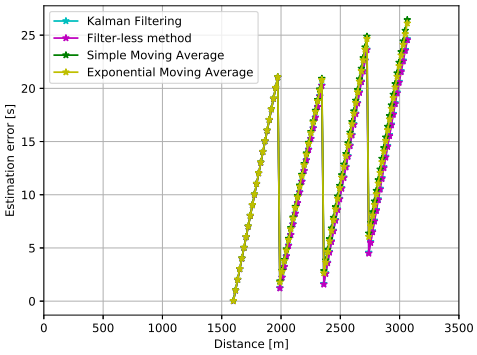

(c) e, d_2 = 1598m, L = 380m.

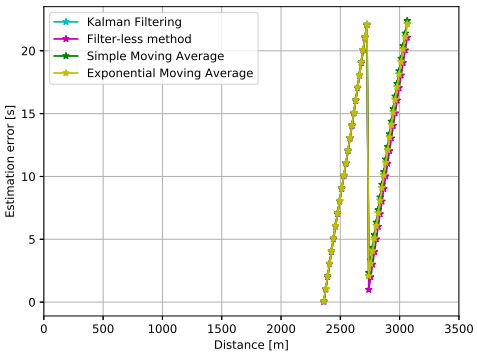

(d) e, d_3 = 2361m, L = 375m.

Fig. 12: Comparison of the estimation errors for different dissemination areas size.

Therefore, as concluded in Section IV-C, the estimation error is a function of dissemination area size L, speed v, and the n index, which allows us to predict, to control, and to bound, this error by adjusting the aforementioned parameters (eq. 12). To better showcase the aforementioned, in Fig. 12 we present the behavior of the estimation error depending on the size of dissemination area at the four considered reference locations, i.e., d_0, d_1, d_2, d_3. In each of these cases, Fig. 12 and Table II show how the estimation error changes for all four reference methods with the change in the size of the dissemination area L.

In Fig. 12a, when the EmV is located at the d_0 distance from the starting point, the size of the dissemination area has a default value, i.e., 1000m. In this case, the RMSE for the Kalman filtering is 23.86s, while it obtains values of 54.30s for the other three techniques. Afterwards, when the EmV moves and reaches the d_1 (travelling 710m from the starting point), Fig. 12b shows that our algorithm adjusted the size of dissemination area in order to decrease the estimation error. The new size becomes 335m, yielding the RMSE of 13.32s, 18.42s, 18.68s, and 18.12s, in case of Kalman filtering, Filter-less method, Simple Moving Average Filter, and Exponential Moving Average Filter, respectively. Results in Fig. 12c and Fig. 12d follow the same trend.

This clearly shows that the correcting behavior or our algorithm is continuously decreasing the estimation error by dynamically adjusting the area size. With the dynamic adjustments of dissemination area sizes, applied by extracting the EmV's speed from the received CAM, as well as the maximum allowed error (threshold), our algorithm is capable of providing more accurate ETA estimations. This is the second advantage of our solution compared to the existing systems.

In addition to the previous analysis, we explored how the estimation error changes for the Moving Average filter (eq. 5) and the Exponential Moving Average filter (eq. 6), in case the window size changes. We observed the three values of the window size, i.e., 5s, 10s, and 50s, and the results show no improvement compared to the Kalman filtering. On the contrary, for some locations in the case study, averaging speed values for longer intervals produced an underestimation of the EmV arrival time.

It is also important to recall that in our proposed solution, vehicles will receive early notifications of an approaching EmV, which will provide them with sufficient time to clear the required lane. In such a solution, the EmV can always select the shortest path or/and the path where it can drive at the maximum allowed speed for emergency systems. Thus, there is no need for collecting long time speed data history to provide an accurate ETA calculation. This is considered as the third advantage of our solution compared to existing systems.

3) Update frequency of CAM notifications: To achieve the third objective of this work, here we present the results we obtained when changing the update frequency of CAM notifications. If we take a look at Fig. 13, it is evident that the estimation error changes with the update frequency of CAMs. However, we need to consider more carefully how significant is the exact difference in estimation error (Fig. 13). The CAM periods shown in Fig. 13, change from 0.1s to 1s, 2s, and 3s, respectively. The respective average MAE values change i) 10.16s, 10.11s, 10.24s, and 10.30s, when using the Kalman filter, ii) 13.33s, 13.17s, 13.33s, and 13.40s, for the Filter-less method, iii) 13.41s, 13.89s, 14.67s, and 15.14, for the Simple Moving Average, and finally iv) 13.40s, 13.81s, 14.48s, and 14.93s, in case of the Exponential Moving Average.

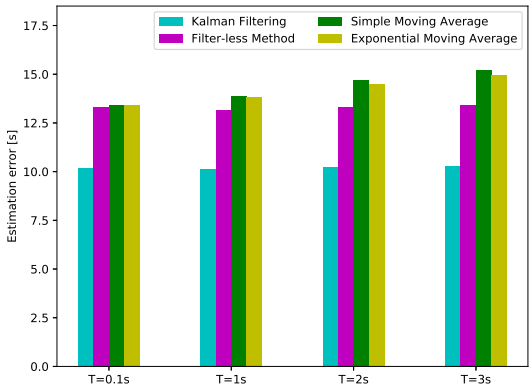

Fig. 13: Comparison of the MAE maximum values obtained for the whole journey of the EmV using different period T for CAM notifications.

We can see that the difference in average MAE values is always lower than 2s. In our particular case, such value is considered small as it does not affect the performance of BSA operation, since the MEC service sends periodic updates to the vehicles in a timely manner, i.e., early enough to clear the lane. For example, if a notification for a civilian vehicle indicates that an EmV is approaching in 2min (which is an ETA value), and EmV arrives in 2min and 2s, or 1min and 58s, such difference in the received ETA will not affect the driver's decision to clear the lane. In addition, the study provided by Toledo and Zohar [49], states that the average duration of lane change on the highways is 5.8s, which means that the driver will need to make a plan on the lane change upfront, and 2s will clearly not play a significant role in this decision. Thus, we can conclude that changing the update frequency of CAM notifications will not significantly affect the estimation accuracy, which means that our algorithm does not require more frequent reception of CAM updates to produce relevant and sufficiently accurate ETA values. If this was not the case, BSA service would be expected to process more messages, thereby consuming more computational resources. Such benefit is essential for deploying BSA service on the MEC platforms, which are usually not resourceful as cloud environments.

4) Complexity of filtering methods: One of the goals of performing the cross-analysis of different reference methods, i.e., the Filter-less method, the Moving Average filter, and the Exponential Moving Average filter, is also to investigate whether a sufficient estimation accuracy can be obtained by using methods with lower complexity and costs compared to the Kalman filter. Thus, by using the Big-O notation, we performed the comparative analysis of the computational time while considering the upper bound of the running time of the algorithms. The results show that all three methods run in $O(n)$ time, where n depends on the number of the considered way-points toward the destination. Regardless of the method type, a longer distance from the destination implies more computational steps, i.e., the linear increase in computational time. On the other side, Kalman Filter is performing the following three steps for each newly received CAM (initial-

ization, prediction, and correction), as it is characterized by a recursive nature, thereby using the output as an input for the next calculation. As expected, this increases the computational time compared to the other three methods. However, despite the increased complexity, Kalman filter provides better results, especially for longer-time predictions. Also, it sustains better stability in the accuracy compared to other methods when the update frequency of CAM notifications changes (Fig. 13). Hence, the complexity vs. accuracy trade-off needs to be carefully studied for any type of application. In our particular case, the computational time is the time needed for our algorithm to re-calculate ETA values for the dynamically defined dissemination areas based on the newly received CAM. The update frequency of CAMs, which can be 1Hz, enables our algorithm to achieve a sufficient level of accuracy (as shown in Fig. 13) and affords it with at least 1s to perform the calculation before new CAM notification arrives. Thus, as such a time gap is sufficient even for the Kalman filtering method, a better prediction accuracy plays a more significant role, making Kalman filtering the most suitable method for our approach.

In addition, it is important to note that the presented analysis is performed considering the highway scenarios. However, we think that the proposed solution can give the same results also when employed within scenarios with non-linear paths in crowded cities, or other urban and rural areas, in view of its reliance on periodic CAM notifications and the self-correcting property of the algorithm. As long as the areas are covered by the 5G mobile network infrastructure, with the MEC system hosting the BSA service, the vehicles encountered on the selected route path will be notified about the arrival of an EmV. Therefore, the vehicles will have enough time to free the required lane. Also, the BSA is being constantly updated with the speed and location of the EmV, while it is heading toward the destination. This real-time speed/location information will be used by the application to evaluate the EmV's progress toward the destination, thus defining new values of ETA, and disseminating accurate results independently of the path linearity. In addition, the application will save and process the location and time information of the EmV for the respective segments, and use this data to update the required parameters in the historical database. As such data shows the behavior of EmVs at different times/days, the BSA application will be able to perform a corresponding statistical analysis to improve the accuracy of the ETA calculation. This advantage makes our solution applicable to any road traffic and scenario.

The dissemination of the ETAs in crowded cities will be performed using smaller cells and smaller dissemination areas size. The vehicles which are covered by this, but are found outside of the selected route path, will filter the ETA information considering the route they are located. A more detailed analysis on this is part of our future work.

VI. Conclusion

In this paper, we introduced the BSA application for providing an early notification of the ETA of an approaching EmV. The ETA is calculated by the BSA service placed within the MEC system. As the ETA algorithm provides the main logic to the BSA application, the performance of this self-correcting algorithm has been analyzed and evaluated in terms of accuracy of ETA estimation. To this end, we incorporated the dynamic definition of the dissemination area size, and we used different forecasting techniques. The real field data measurements obtained in a realistic environment, such as the Smart Highway testbed in Antwerp, Belgium, are used for developing the model, as well as for required analysis, evaluation, and comparison.

First, the developed algorithm is being periodically updated with the EmV speed and location information, to follow the flow and fast changes in the traffic, and it uses these input values for its self-correcting behavior towards improving the ETA accuracy.

Second, the developed algorithm analyzes the dependency between the estimation error, the dissemination area size, and the EmV speed, while heading to the emergency case. As a result, the algorithm dynamically allocates the dissemination areas, and adjusts their size. This newly added feature to our proposed BSA algorithm maintains the estimation error under a defined threshold, required for an emergency situation.

To study the accuracy of the ETA estimation achieved by different methods, we made a comparison between i) Kalman filter, ii) one-step speed values from CAM referred to as Filter-less method, iii) the average speed values using Moving Average filter, and iv) the Exponential Moving Average filter. According to our results, the Kalman filter proved to produce the most optimal result by providing the highest estimation accuracy, compared to the other prediction methods. This Kalman accuracy gain becomes even more relevant when the algorithm needs to predict ETA values for longer distances.

Although the computational complexity of the Kalman Filter is higher compared to other methods because of its recursive nature, our experimentation has shown that the computational time of Kalman filter has the same order of magnitude as in case of the other methods, resulting in an increase in time that not significant. In addition, we can reduce the CAM input frequency (increase CAM period from 1s to 2s, or 3s), and still, Kalman filter sustains better stability in the accuracy compared to other methods.

With such BSA system, when the ETA notification is beyond the audio and visual range of the EmV, drivers have enough time to take the required actions and clear the lane. At the same time, the EmV can always select the shortest path toward the destination and drive at the maximum allowed speed for emergency systems. As a result, the proposed solution is expected to not only improve the road safety, but also to enhance the mission success and response time of emergency responders.

Acknowledgment

This work has been funded by the European Union Horizon-2020 Project 5G-CARMEN under Grant Agreement 825012. The views expressed are those of the authors and do not necessarily represent the project.

References

[1] F. Z. Yousaf, M. Bredel, S. Schaller, and F. Schneider, "NFV and SDN—Key Technology Enablers for 5G Networks," *IEEE Journal on Selected Areas in Communications*, vol. 35, no. 11, pp. 2468–2478, 2017, doi: http://dx.doi.org/10.1109/JSAC.2017.2760418.

[2] R. Aringhieri, G. Carello, and D. Morale, "Ambulance location through optimization and simulation : the case of milano urban area," 2007, doi: http://dx.doi.org/.

[3] R. Sánchez-Mangas, A. García-Ferrrer, A. de Juan, and A. M. Arroyo, "The probability of death in road traffic accidents. how important is a quick medical response?" *Accident Analysis & Prevention*, vol. 42, no. 4, pp. 1048–1056, 2010, doi: http://dx.doi.org/10.1016/j.aap.2009.12.012.

[4] R. B. Vukmir, "Survival from prehospital cardiac arrest is critically dependent upon response time," *Resuscitation*, vol. 69, no. 2, pp. 229–234, 2006, doi: http://dx.doi.org/10.1016/j.resuscitation.2005.08.014.

[5] M. Poulton, A. Noulas, D. Weston, and G. Roussos, "Modeling metropolitan-area ambulance mobility under blue light conditions," *IEEE Access*, vol. 7, pp. 1390–1403, 2019, doi: http://dx.doi.org/10.1109/ACCESS.2018.2886852.

[6] N. Smith, "A National Perspective on Ambulance Crashes and Safety - Guidance from the National Highway Traffic Safety Administration on Ambulance Safety for Patients and Providers," *EMS Report*, 2015, online [Available]:https://pubmed.ncbi.nlm.nih.gov/26521402/.

[7] K. Donoughe, J. Whitestone, and H. Gabler, "Analysis of Firetruck Crashes and Associated Firefighter Injuries in the United States," *Annals of advances in automotive medicine / Annual Scientific Conference. Association for the Advancement of Automotive Medicine. Association for the Advancement of Automotive Medicine. Scientific Conference*, vol. 56, pp. 69–76, 10 2012, online [Available]:https://www.ncbi.nlm.nih.gov/pmc/articles/PMC3503424/.

[8] X. Yang, L. Liu, N. Vaidya, and F. Zhao, "A vehicle-to-vehicle communication protocol for cooperative collision warning," in *The First Annual International Conference on Mobile and Ubiquitous Systems: Networking and Services, 2004. MOBIQUITOUS 2004.*, 2004, pp. 114–123, doi:http://dx.doi.org/10.1109/MOBIQ.2004.1331717.

[9] ETSI, "Multi-Access Edge Computing (MEC); Framework and Reference Architecture," *ETSI ISG MEC, ETSI GS MEC 003 V2.1.1*, 2019, online [Available]: https://www.etsi.org/deliver/etsi_gs/MEC/001_099/003/02.01.01_60/gs_MEC003v020101p.pdf.

[10] ——, "Intelligent Transport Systems (ITS); Vehicular Communications; Basic Set of Applications; Part 2: Specification of Cooperative Awareness Basic Service," *ETSI ISG ITS, ETSI EN 302 637-2 V1.4.1*, 2019, online [Available]:https://www.etsi.org/deliver/etsi_en/302600_302699/30263702/01.03.02_60/en_30263702v010302p.pdf.

[11] ETSI., "Intelligent Transport Systems (ITS); Vehicular Communications; Basic Set of Applications; Part 3: Specification of Decentralized Environment Notification Basic Service," *ETSI ISG ITS, ETSI EN 302 637-3 V1.3.0*, 2018, online [Available]:https://www.etsi.org/deliver/etsi_en/302600_302699/30263703/01.02.01_30/en_30263703v010201v.pdf.

[12] R. Halili, F. Z. Yousaf, N. Slamnik-Kriještorac, G. M. Yilma, M. Liebsch, E. de Britto e Silva, S. A. Hadiwardoyo, R. Berkvens, and M. Weyn, "Leveraging mec in a 5g system for enhanced back situation awareness," in *2020 IEEE 45th Conference on Local Computer Networks (LCN)*, 2020, pp. 309–320, doi: http://dx.doi.org/10.1109/LCN48667.2020.9314838.

[13] R. E. Kalman, "A New Approach to Linear Filtering and Prediction Problems," in *Transaction of the Asme Journal of Basic*, 1960, online [Available]:http://www.unitedthc.com/DSP/Kalman1960.pdf.

[14] R. Aringhieri, G. Carello, and D. Morale, "Ambulance location through optimization and simulation: the case of milano urban area," in *XXXVIII Annual Conference of the Italian Operations Research Society Optimization and Decision Sciences:1-29*, 2007.

[15] J. Nicholl, J. West, S. Goodacre, and J. Turner, "Tg," *Emergency Medicine Journal*, vol. 24, no. 9, pp. 665–668, 2007, doi:http://dx.doi.org/10.1136/emj.2007.047654.

[16] J. Pell, J. Sirel, A. Marsden, I. Ford, and S. Cobbe, "Effect of Reducing Ambulance Response Times on Deaths from out of Hospital Cardiac Arrest: Cohort Study," *BMJ (Clinical research ed.)*, vol. 322, pp. 1385–8, 07 2001, doi:http://dx.doi.org/10.1136/bmj.322.7299.1385.

[17] A. P. Iannoni, R. Morabito, and C. Saydam, "An optimization approach for ambulance location and the districting of the response segments on highways," *European Journal of Operational Research*, vol. 195, no. 2, pp. 528–542, June 2009, doi: https://ideas.repec.org/a/eee/ejores/v195y2009i2p528-542.html.

[18] M. Poulton, A. Noulas, D. Weston, and G. Roussos, "Modeling Metropolitan-Area Ambulance Mobility Under Blue Light Conditions," *IEEE Access*, vol. 7, pp. 1390–1403, 2019, doi: http://dx.doi.org/10.1109/ACCESS.2018.2886852.

[19] A. Emami, M. Sarvi, and S. Bagloee, "Using Kalman filter algorithm for short-term traffic flow prediction in a connected vehicle environment," *Journal of Modern Transportation*, 07 2019, doi:http://dx.doi.org/10.1007/s40534-019-0193-2.

[20] Jiann-Shiou Yang, "Travel time prediction using the gps test vehicle and kalman filtering techniques," in *Proceedings of the 2005, American Control Conference, 2005.*, 2005, pp. 2128–2133 vol. 3, doi:http://dx.doi.org/10.1109/ACC.2005.1470285.

[21] W. Min, L. Yu, P. Chen, M. Zhang, Y. Liu, and J. Wang, "On-Demand Greenwave for Emergency Vehicles in a Time-Varying Road Network With Uncertainties," *IEEE Transactions on Intelligent Transportation Systems*, vol. 21, no. 7, pp. 3056–3068, 2020, doi:http://dx.doi.org/10.1109/TITS.2019.2923802.

[22] K. Nellore and G. Hancke, "A Survey on Urban Traffic Management System Using Wireless Sensor Networks," *Sensors*, vol. 16, p. 157, 01 2016, doi:http://dx.doi.org/10.3390/s16020157.

[23] S. Rimer and G. Hancke, "Actor Coordination Using Info-Gap Decision Theory in Wireless Sensor and Actor Networks," *IJSNet*, vol. 10, pp. 177–191, 10 2011, doi:http://dx.doi.org/10.1504/IJSNET.2011.042769.

[24] S. Joerer, B. Bloessl, M. Segata, C. Sommer, R. L. Cigno, A. Jamalipour, and F. Dressler, "Enabling situation awareness at intersections for ivc congestion control mechanisms," *IEEE Transactions on Mobile Computing*, vol. 15, no. 7, pp. 1674–1685, 2016, doi:http://dx.doi.org/10.1109/TMC.2015.2474370.

[25] H. Nguyen and H. Jeong, "Mobility-Adaptive Beacon Broadcast for Vehicular Cooperative Safety-Critical Applications," *IEEE Transactions on Intelligent Transportation Systems*, vol. 19, no. 6, pp. 1996–2010, 2018, doi:http://dx.doi.org/10.1109/TITS.2017.2775287.

[26] A. Senart, M. Bouroche, and V. Cahill, "Modelling an Emergency Vehicle Early-warning System using Real-time Feedback," *IJIIDS*, vol. 2, pp. 222–239, 01 2008, doi:http://dx.doi.org/10.1504/IJIIDS.2008.018256.

[27] N. Kapileswar, P. V. Santhi, V. K. R. Chenchela, and C. H. V. S. Prasad, "A Fast Information Dissemination System for Emergency Services over Vehicular Ad Hoc Networks," in *2017 International Conference on Energy, Communication, Data Analytics and Soft Computing (ICECDS)*, 2017, pp. 236–241, doi:http://dx.doi.org/10.1109/ICECDS.2017.8389862.

[28] T. Johnson, "Emergency Vehicle Notification System," *U.S. Patent 7,397,356.*, 2005, online [Available]:https://patents.google.com/patent/US7397356.

[29] S. A. Hadiwardoyo, S. Patra, C. T. Calafate, J.-C. Cano, and P. Manzoni, "An intelligent transportation system application for smartphones based on vehicle position advertising and route sharing in vehicular ad-hoc networks," *Journal of Computer Science and Technology*, vol. 33, no. 2, pp. 249–262, 2018, doi:https://doi.org/10.1007/s11390-018-1817-4.

[30] A. Metzner and T. Wickramarathne, "Exploiting Vehicle-to-Vehicle Communications for Enhanced Situational Awareness," in *2019 IEEE Conference on Cognitive and Computational Aspects of Situation Management (CogSIMA)*, 2019, pp. 88–92, doi:http://dx.doi.org/10.1109/COGSIMA.2019.8724309.

[31] Y. Moroi and K. Takami, "A Method of Securing Priority-Use Routes for Emergency Vehicles using Inter-Vehicle and Vehicle-Road Communication," in *2015 7th International Conference on New Technologies, Mobility and Security (NTMS)*, 2015, pp. 1–5, doi:http://dx.doi.org/10.1109/NTMS.2015.7266466.

[32] J. Zhang and K. B. Letaief, "Mobile Edge Intelligence and Computing for the Internet of Vehicles," *Proceedings of the IEEE*, vol. 108, no. 2, pp. 246–261, 2020, doi: https://doi.org/10.1109/JPROC.2019.2947490.

[33] S. A. A. Shah, E. Ahmed, M. Imran, and S. Zeadally, "5G for Vehicular Communications," *IEEE Communications Magazine*, vol. 56, no. 1, pp. 111–117, Jan 2018, doi:http://dx.doi.org/10.1109/MCOM.2018.1700467.

[34] K. Abboud, H. A. Omar, and W. Zhuang, "Interworking of DSRC and Cellular Network Technologies for V2X Communications: A Survey," *IEEE Transactions on Vehicular Technology*, vol. 65, no. 12, pp. 9457–9470, 2016, doi: https://doi.org/10.1109/TVT.2016.2591558.

[35] N. Slamnik-Kriještorac, H. C. Carvalho de Resende, C. Donato, S. Latré, R. Riggio, and J. Marquez-Barja, "Leveraging Mobile Edge Computing to Improve Vehicular Communications," in *2020 IEEE 17th Annual Consumer Communications Networking Conference (CCNC)*, 2020, pp. 1–4, doi:http://dx.doi.org/10.1109/CCNC46108.2020.9045698.

[36] B. Carr, M. Caplan, J. Pryor, and C. Branas, "A meta-analysis of prehospital care times for trauma." *official journal of the National Association of EMS Physicians and the National Association of State EMS Directors*, vol. 7, pp. 198–206, 2006, doi: http://dx.doi.org/10.1080/10903120500541324.

[37] L. Aboueljinane, E. Sahin, and Z. Jemai, "A review on simulation models applied to emergency medical service operations," *Computers & Industrial Engineering*, vol. 66, no. 4, pp. 734–750, 2013, doi: http://dx.doi.org/10.1016/j.cie.2013.09.017.

[38] Vanetza, "Vanetza - Open Source ETSI C-ITS protocol suite," 2020, online [Available]:http://http://www.vanetza.org/, Last accessed on 2020-6-1.

[39] S. I. Chien and C. M. Kuchipudi, "Dynamic travel time prediction with real-time and historic data," *Journal of Transportation Engineering*, vol. 129, no. 6, pp. 608–616, 2003, doi: https://ascelibrary.org/doi/abs/10.1061/(ASCE)0733-947X(2003)129:6(608).

[40] Y. Pan, L. Sun, and M. Ge, "Finding reliable shortest path in stochastic time-dependent network," *Procedia - Social and Behavioral Sciences*, vol. 96, pp. 451–460, 2013, intelligent and Integrated Sustainable Multimodal Transportation Systems Proceedings from the 13th COTA International Conference of Transportation Professionals (CICTP2013). [Online]. Available: https://www.sciencedirect.com/science/article/pii/S1877042813021794

[41] X. Wu and Y. M. Nie, "Modeling heterogeneous risk-taking behavior in route choice: A stochastic dominance approach," *Procedia - Social and Behavioral Sciences*, vol. 17, pp. 382–404, 2011, papers selected for the 19th International Symposium on Transportation and Traffic Theory.

[Online]. Available: https://www.sciencedirect.com/science/article/pii/S1877042811010822

[42] Y. Fan and Y. Nie, "Optimal routing for maximizing the travel time reliability," *Networks and Spatial Economics*, vol. 6, no. 3-4, pp. 333–344, 2006, doi: https://doi.org/10.1007/s11067-006-9287-6.

[43] J. Marquez-Barja, B. Lannoo, D. Naudts, B. Braem, V. Maglogiannis, C. Donato, S. Mercelis, R. Berkvens, P. Hellinckx, M. Weyn *et al.*, "Smart Highway: ITS-G5 and C2VX based testbed for vehicular communications in real environments enhanced by edge/cloud technologies," in *EuCNC2019, the European Conference on Networks and Communications*, 2019, pp. 1–2, available [Online]:https://biblio.ugent.be/publication/8642435.

[44] A. B. Patel, N. M. Waters, I. E. Blanchard, C. J. Doig, and W. A. Ghali, "A validation of ground ambulance pre-hospital times modeled using geographic information systems," *International Journal of Health Geographics*, vol. 11, no. 1, p. 1, 2012. [Online]. Available: InternationalJournalofHealthGeographics

[45] A. Shalaby and A. Farhan, "Prediction Model of Bus Arrival and Departure Times Using AVL and APC Data," *Journal of Public Transportation*, vol. 7, 03 2004, doi:http://dx.doi.org/10.5038/2375-0901.7.1.3.

[46] B. Yu, Z.-Z. Yang, K. Chen, and B. Yu, "Hybrid model for prediction of bus arrival times at next station," *Journal of Advanced Transportation*, vol. 44, no. 3, pp. 193–204, 2010. [Online]. Available: https://onlinelibrary.wiley.com/doi/abs/10.1002/atr.136

[47] F. Sun, Y. Pan, J. White, and A. Dubey, "Real-time and predictive analytics for smart public transportation decision support system," in *2016 IEEE International Conference on Smart Computing (SMARTCOMP)*, 2016, pp. 1–8, doi: http://dx.doi.org/10.1109/SMARTCOMP.2016.7501714.

[48] A. Bensky, *Wireless Positioning Technologies and Applications, Second Edition*, 2nd ed. Artech House, 2016.

[49] T. Toledo and D. Zohar, "Modeling duration of lane changes," *Transportation Research Record*, vol. 1999, no. 1, pp. 71–78, 2007, doi: http://dx.doi.org/10.3141/1999-08.

Rreze Halili is a PhD Researcher at the University of Antwerp and IDLab - a core research group of IMEC. She received her Bachelor of Science in Electrical Engineering – Telecommunications and Master of Science in Telecommunications from the University of Prishtina, Faculty of Electrical and Computer Engineering, in 2011 and 2014 respectively. She worked as Teaching Assistant at the University of Prishtina, and was a research intern at Robert Bosch Research in Germany. Her research interests involve vehicle localization using wireless communication and satellite technologies, radio wave propagation, reliable and safe wireless cellular communications.

Faqir Zarrar Yousaf is a Senior Researcher at NEC Laboratories Europe, Germany. He completed his PhD from TU Dortmund, Germany. His current research interest is on NFV/SDN in the context of 5G networks. He is also an active contributor to ETSI ISG NFV standards organization where he holds Rapporteurship for six work-items. He has extensive experience in the design, development, modeling, simulation and prototyping of communication systems and protocols for optimizing overall network performance. He has 04 granted patent and 15 filed patents while his research work has been published in several peer reviewed journals, conferences and book chapters.

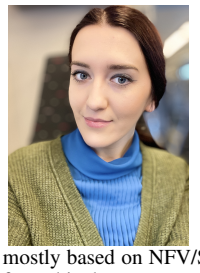

Nina Slamnik-Kriještorac is currently a PhD researcher in the field of Applied Engineering Sciences, at the University of Antwerp and the IMEC research center in Belgium. She obtained her Master degree in telecommunications engineering at Faculty of Electrical Engineering, University of Sarajevo, Bosnia and Herzegovina, in July 2016. In the period from 2016 to 2018, she worked as a Teaching Assistant at University of Sarajevo. She authored or co-authored several publications in journals and international conferences. Her current research is mostly based on NFV/SDN-based network architectures with edge computing for vehicular systems, and the management and orchestration of the flexible and programmable next generation end-to-end network resources and services.

Girma M. Yilma is Research Engineer at NEC Laboratories Europe in Heidelberg, Germany. He received his B.Sc. (2010) in Electrical and Computer Engineering from Addis Ababa University, and M.Sc. (2016) in Telecommunications Engineering from University of Trento, Italy. His current research interest is focused around NFV MANO, Orchestration, Cloud Native Network Orchestration, NFV/SDN related technologies in the context of 5G network architecture and operations.

Marco Liebsch is chief researcher at NEC Laboratories Europe GmbH and is working in the area of 5G mobility management, mobile edge computing and content distribution, mobile cloud networking, and software-defined networking. He received his Ph.D. degree from University of Karlsruhe, Germany, in 2007. He worked in different EU research projects and is contributing to standards in the IETF, ETSI and 3GPP. He has a long record of IETF contributions as well as RFC, journal and conference publications.

Rafael Berkvens is a postdoctoral researcher at the University of Antwerp, Belgium. He received his Masters degree in Applied Engineering: Electronics-ICT from the University of Antwerp, in 2012. He received his Ph.D. degree on indoor location information quantification from the same university in 2017, working at the IDLab – imec research group. He currently serves as researcher and Teaching Assistant at the University of Antwerp.

Maarten Weyn received his Ph.D. in Computer Science from the University of Antwerp, Belgium. He is a Professor at the University of Antwerp. Maarten is instructor at the LoraWAN Academy on the topic of localization and lecturer in a few courses on Coursera on Embedded IoT systems. His research in the imec-IDlab research group focuses on ultra-low power sensor communication and embedded systems, sub 1-Ghz communication, sensor processing and localization. Most of his projects are in close collaboration with industry. He is the co-founder of the spin-offs Aloxy, CrowdScan and AtSharp, involved in the creation of the spin-offs 1OK and Viloc, director of the Dash7 Alliance, IARIA Fellow and initiator of the Open Source Stack OSS-7.